Progress In Electromagnetics Research Letters, Vol. 96, 121–128, 2021

Ultraviolet Vortex Generation through All-Dielectric Nano-Antennas for Free Space Optical Communication

Arslan Asim*

Abstract—Metamaterials have revolutionized the research in conventional electromagnetics. They display unique properties which can be used for the manipulation of electromagnetic waves in unexpected ways. In this research, a diamond nano-antenna is designed and optimized using the CST Microwave Studio, which uses Finite Difference Time Domain (FDTD) method. The designed unit cell shows high polarization conversion rates (PCR) for ultraviolet (UV) frequencies (especially the UV-B band) whilst covering Panchatram-Berry (PB) phase. The unit cell is then used to design metasurfaces that generate light beams carrying Orbital Angular Momentum (OAM) of different orders. Through the design of two dimensional metamaterial surfaces, the behavior of electromagnetic beams can be changed on subwavelength scale. This has led to a number of applications related to nanotechnology. A vortex beam carries Orbital Angular Momentum (OAM) which has played a vital role in increasing the bandwidth and data rate of optical communication systems. Therefore, OAM beams having different topological charges have been generated at 294 nm to propose an improvement in Free Space Optical (FSO) communication. Optical links also function as a suitable substitute for applications where Radio Frequency (RF) communications may not be effective. The proposed theoretical model is expected to open new horizons in optical communication by incorporating the use of nanoscale devices with high efficiencies in the ultraviolet regime.

1. INTRODUCTION

Light carries linear momentum as supported by Poynting's theory of electromagnetic radiation pressure and momentum density. Subsequently, Poynting also explained the spin angular momentum, which is linked to the circular polarization of light. However, another closely related property of light named 'Orbital Angular Momentum (OAM)' was explained years later in 1992 [1], which is due to helical phase fronts of electromagnetic waves. Orbital angular momentum has since been an area of keen interest for researchers. Nowadays, OAM beams are famously known as vortex beams.

Metamaterials have opened up a completely new dimension in the field of optics because they display unique characteristics when electromagnetic waves interact with them. The word 'metamaterials' describes the class of artificially engineered materials that display properties not commonly found in naturally occurring materials. In this regard, metasurfaces have been under discussion for quite some time now. Metasurfaces stem from the idea of planar optics/photonics [2]. They are so thin that they are considered as two-dimensional surfaces. They consist of nano-antennas which can change the properties (like polarization, phase, etc.) of the incident beam and result in the achievement of different phenomena on nanoscale. These nano-antennas are sub-wavelength structures that provide resonance for particular frequencies.

Since metasurfaces are small compared to the traditional devices, they offer a suitable alternative to be used in opto-electronic devices. Metasurfaces have initially been linked to plasmonic materials, but

Received 2 January 2021, Accepted 9 February 2021, Scheduled 17 February 2021
* Corresponding author: Arslan Asim (arslan.asim@umt.edu.pk).
The author is with the Institute of Aviation Studies, University of Management and Technology (UMT), Lahore, Pakistan.

plasmonic nanostructures suffer from higher losses and heating. They may also not be compatible with complementary metal oxide semiconductor fabrication processes. Therefore, in this work, focus has been given to optically resonant 'dielectric' nanostructures since they can give higher device efficiency [3, 4]. The primary focus of this work is on the use of diamond nano-antennas.

Over the past years, generation of vortex beams through different novel methods has been introduced. Some of the conventional methods include spiral phase plate [5, 6], spiral parabolic antenna, and circular antenna array [7–9]. However, the traditional techniques are bulky and difficult to integrate in nanoscale optoelectronic devices. Therefore, metasurfaces are presented as a possible alternative to this problem.

The current focus of research is on the use of nanotechnology to generate vortex beams. For example, Yue et al. [10] recently demonstrated a method of generating vector vortex beams using a single plasmonic metasurface. They used gold nanorods to design a reflection-based metasurface for vortex generation at 697 nm. Similar works on plasmonic metasurfaces' use in vortex beam generation include [11–14]. In contrast with the discussed approaches, optical vortex beams have also been demonstrated through the use of dielectrics, which promise a higher efficiency. The progress reported in [15–19] is based on the use of dielectric nanostructures for optical vortex generation.

The key features of the quoted works are mentioned in Table 1. The generation of ultraviolet vortex beams still seems a less discovered topic, whose importance cannot be ignored in terms of the wide variety of applications associated with vortex beams [20].

The primary motivation behind this work is optical communication, particularly free space optical communication (FSOC) in the ultraviolet regime. The importance of Radio Frequency (RF) communication has been well acknowledged till today, but factors like attenuation, energy efficiency restrictions, and RF interference can cause the RF communication links to become ineffective [21]. Under such circumstances, Optical Wireless (OW) links can provide a cost effective solution because they are immune to electromagnetic interference and free from licensing requirements. Links using ultraviolet wavelengths have been under considerable attention for the past half century. The area of ultraviolet communication dates back to the 1960's when the UV-C band (200–280 nm) was essentially introduced as a means of Non Line of Sight (NLOS) communication. Recently, the UV-B wavelengths (280–315 nm) have also been proposed as potential candidates for optical communications. In one of the latest works, a communication link was successfully shown with a UV-B wavelength of 294 nm [22].

Optical vortex beams can be used as information carriers in ultraviolet communication systems since they provide an alternative degree of freedom known as mode/spatial division multiplexing (MDM/SDM). This is especially important in terms of bandwidth of operation and data rate. Therefore, OAM beams have played a phenomenal role in bringing about the terabit revolution in optical communications [23–25].

2. DESIGN AND ANALYSIS

An important part of this work revolves around the study of material properties that can provide high efficiency for ultraviolet region. Diamond appears to be the right choice since it shows resonance on the incidence of ultraviolet frequencies. Figure 1 presents the dielectric dispersion properties of the materials used in this work [26].

The meta-atom shape used is a nano-brick, and the mathematical description for it is provided. The nano-brick can be rotated to tailor the wave-fronts of the incident electromagnetic waves. The rotation angle of the nano-brick can be represented as θ. The relation of the rotation angles with the transmitted electromagnetic beam is explained through the expressions given below. The rotation matrix of the nanobrick is

$$R(\theta) = \begin{bmatrix} \cos\theta & \sin\theta \\ -\sin\theta & \cos\theta \end{bmatrix} \tag{1}$$

The transmission matrix T' can be evaluated as [27]

$$T' = R(-\theta) \cdot T \cdot R(\theta) = \begin{bmatrix} \cos\theta & \sin\theta \\ -\sin\theta & \cos\theta \end{bmatrix} \begin{bmatrix} T_{11} & 0 \\ 0 & T_{22} \end{bmatrix} \begin{bmatrix} \cos\theta & \sin\theta \\ -\sin\theta & \cos\theta \end{bmatrix} \tag{2}$$

$$\vec{E}_t = T' \cdot \vec{E}_{in} \tag{3}$$

Table 1. Comparison of the work presented in the paper with other contemporary works.

REF.	GEOMETRY	MATERIAL	WAVE-LENGTH	META-SURFACE	APPLICATION
[10]	Nanorod	Gold with silicon dioxide	697 nm	Reflective	Free space communication
[11]	Dolphin	Silver with silica	321 nm, 660 nm, 448 nm	Transmissive	Communication, bioscience
[12]	Nanoslit	Gold with glass	633 nm	Transmissive	Quantum information processing, particle manipulation, communication
[13]	Nanoantennas	Gold with silicon dioxide	800–950 nm	Reflective	Particle trapping, communication
[14]	I shape	Copper with F4B	5.2 GHz (57.6524 mm), 10.5–12 GHz (24.9827–28.55166 mm)	Reflective	Communication
[15]	Elliptical resonator	Silicon with fused silica	1300–1700 nm	Transmissive	Communication
[16]	Elliptical nanopillar	Silicon with fused silica	1500–1600 nm	Reflective	Communication
[17]	Cylindrical nanopillar	Hydrogenated amorphous silicon (A-Si:H) with silicon dioxide	632.8 nm	Transmissive	On-chip utilization
[18]	Cylindrical nanopillar	Hydrogenated amorphous silicon (A-Si:H) with silicon dioxide	633 nm	Transmissive	Optical manipulation, optical alignment, laser fabrication, imaging, and laser machining
[19]	Meta-Reflect Array	Silicon with silver ground plane	1500–1600 nm	Reflective	Metasurface-based devices for high frequencies
This work	Nanobar	Diamond with silicon dioxide	294 nm	Transmissive	Free space Communication

$$\vec{E}_{in} = \vec{E}_{LCP} = \frac{1}{\sqrt{2}} \begin{bmatrix} 1 \\ i \end{bmatrix} \tag{4}$$

$$\vec{E}_t = \frac{T_{11} + T_{22}}{2} \vec{E}_{LCP} + \frac{T_{11} - T_{22}}{2} e^{i2\theta} \vec{E}_{RCP} \tag{5}$$

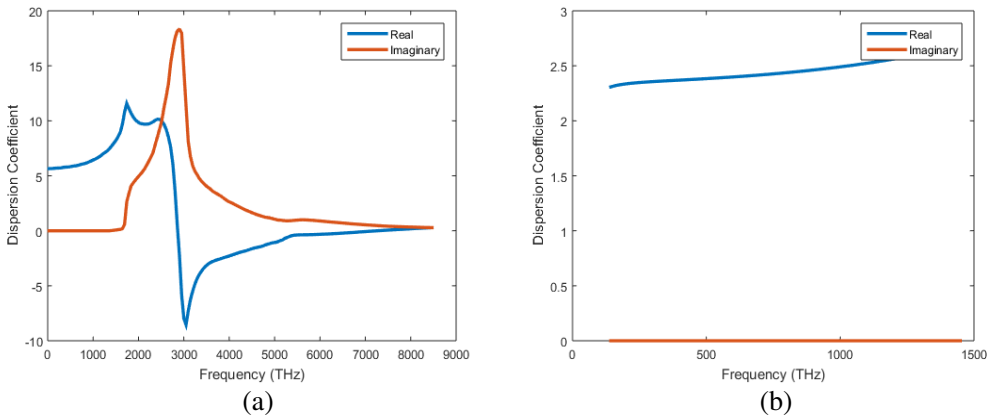

Figure 1. Material dispersion parameters of (a) diamond and (b) silicon dioxide used in this work.

$\vec{E}_{in}$ is the polarization of the incident beam. In this case, it is left circularly polarized, as expressed by the Jones vector. Solving $\vec{E}_t$ gives us an interesting solution. The transmitted beam ($\vec{E}_t$) comprises two components. The nanobrick converts incident Left Circular Polarization ($\vec{E}_{LCP}$) beam into Right Circular Polarization ($\vec{E}_{RCP}$) accompanied by a phase shift equal to twice of the rotation angle of the nanobrick. A part of the incident polarization can be seen on the transmitted side as well. T_{11} and T_{22} represent the transmitted co-polarization intensities.

An important part of this work is the design of the nanometer sized unit cell which has been further used to design the metasurfaces. Figure 2 shows the nano-structure designed in this work. The metasurfaces, proposed in this work, consist of a large number of such unit cells with different rotation angles. The rotation angles of this unit cell determine the phase and shape of the transmitted beam. The unit cell shown not only serves the required function of shaping the electromagnetic beams, but also displays high efficiency in the targeted region. The dimensions of the optimized unit cell have been finalized to suit the particular application. The length (L) = 150 nm, width (W) = 55 nm, and height (H) = 325 nm are the dimensions of the diamond brick. The periodic dimensions of the substrate (silicon dioxide) are $px = py = 205$ nm.

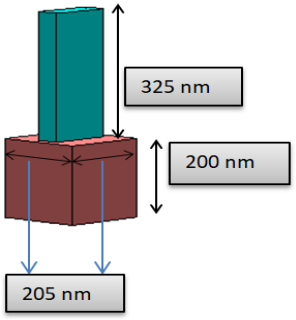

Figure 2. Diamond meta-atom with silicon dioxide substrate.

The designed unit cell provides high Polarization Conversion Rate (PCR) for ultraviolet frequencies. PCR indicates the ratio of the converted cross polarization intensity (I_{cross}) compared to the total intensity of co-polarization and cross polarization ($I_{co} + I_{cross}$). High values of PCR provide effective results at the targeted wavelength.

$$PCR = I_{cross}/(I_{co} + I_{cross}) \tag{6}$$

The response of the nano-antenna for the ultraviolet wavelengths has been shown in Figure 3. Figure 3(a) indicates the intensity of converted cross-polarized electromagnetic beam whereas Fig. 3(b) indicates

the intensity of the co-polarized beam. It can be seen that tremendously high efficiencies have been achieved, through this unit cell, in the ultraviolet regime whilst also converting the incident polarization. The achieved efficiencies are as high as 90%. The targeted UV-B wavelength lies in the range of very high efficiency response. This provides the motivation behind the design of ultraviolet metasurfaces through this particular unit cell. Figure 4 further illustrates these significant features of the unit cell design. The PCR and phase coverage at 294 nm are depicted in Figure 3 as well. The unit cell can be seen to show high values of PCR for all rotation angles at 294 nm. This plays a pivotal role in the design of metasurfaces because different rotation angles of the unit cell have been used in the design to generate the required phenomenon of vortex beams. Also, it is noteworthy that Panchatram-Berry phase control can be achieved through the unit cell design parameters. For different angles of the unit cell, the phase changes in a fashion that it covers a range of 2π. This is also depicted by phase diagrams reported later in the paper.

Further, metasurfaces have been designed with 50×50 meta-atoms, which means that the overall size of each metasurface is 105.0625 μm^2 (10.25 µm by 10.25 µm). The designed metasurfaces have been simulated using CST Microwave Studio which uses Finite Difference Time Domain (FDTD) to provide electromagnetic solutions. The time domain solutions match with the expected plots. The phase function for the metasurfaces is given below:

$$\Phi = k_0 \left(\sqrt{F^2 + x^2 + y^2} - F \right) + m \tan^{-1}(y/x) \tag{7}$$

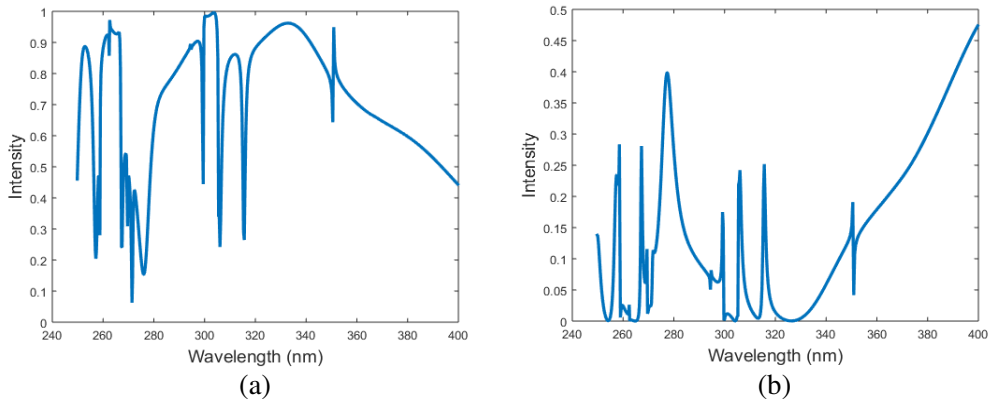

Figure 3. Transmitted co-polarization (a) and cross-polarization, (b) intensities of the diamond unit cell.

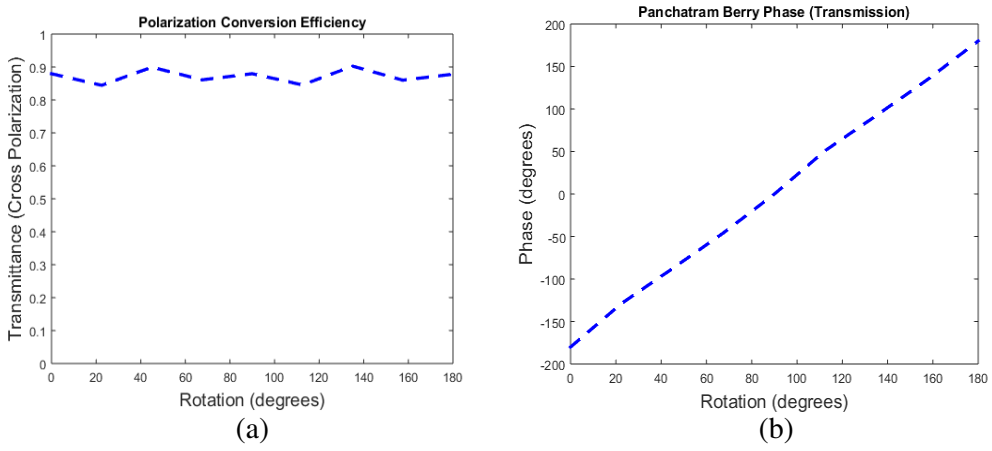

Figure 4. (a) Transmittance plotted against the degrees of rotation of the unit cell, (b) Panchatram Berry (PB) phase of the unit cell.

where F and m represent focal length and topological charge of the vortex beam, respectively. Φ determines the phase profile of the metasurface and is governed by the rotation angles of the nanobricks. The simulation results for $m = 0, 2$ and 4 have been reported in the results.

3. RESULTS

When $m = 0$, the metasurface generates a zero order vortex beam. A zero order vortex beam can also be referred to as a meta-lens. Meta-lens has a lot of applications in planar optics. In fact, they constitute one of the most prominent ideas in this field.

Figure 5(a) shows the resulting electric field intensities. It depicts how the incident plane wave has been converged to a single focal point. The results of the 2D (x-y) electric field monitor have clearly proved that the proposed metasurface design has resulted in electric field concentrating at one point. Figure 5(b) shows the phase along the normal to the x-y plane monitor. Complete phase control has been achieved as promised by the unit cell design.

Metasurfaces have also been designed for vortex beams with orders 2 and 4. The orders were chosen in a way to distinguish the working principle of metasurfaces in relation with the Orbital Angular Momentum. Results for those vortex beams are as given below.

The comparative results provide a lot of insight into the nature of vortex beams. Figures 6(a) and (b) show how vortex beams look when being seen through cross-sections of x-y electric field monitors. The characteristic donut shape of the vortex beams can be clearly observed since the intensity of the electric beam is almost zero in the middle of the beam. It can be noticed that as the topological charge increases, the donut of the vortex beam becomes larger as Fig. 6(b) shows a bigger shape than Fig. 6(a). Phase depiction of the vortex beams is also presented in Figure 6(c).

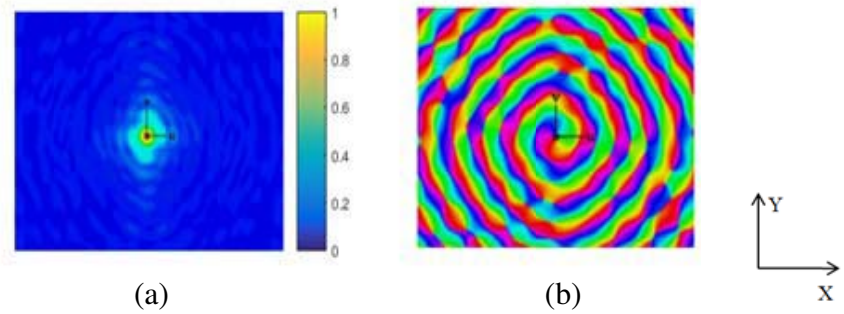

Figure 5. (a) Electric field distribution behind a meta-lens, (b) phase distribution of normal component beyond a meta-lens.

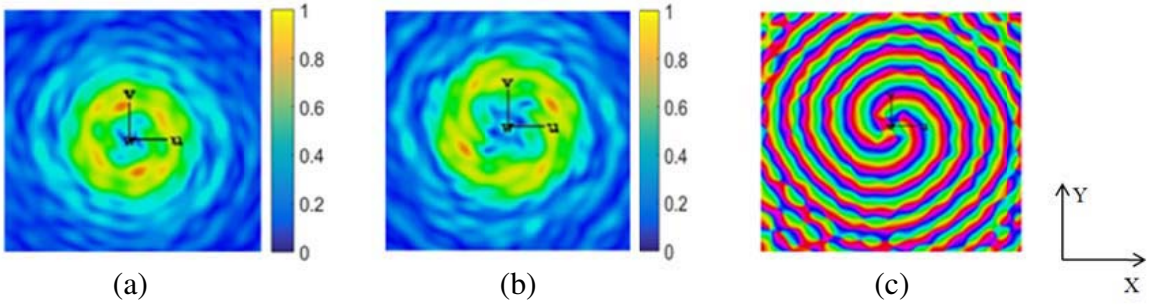

Figure 6. (a) $m = 2$, (b) $m = 4$ vortex beams' electric field distribution, (c) phase (Normal) associated with vortex beams.

4. CONCLUSION

This work has discussed the problem of optical communication in the ultraviolet regime using metamaterials. Optical communication has presented itself as a strong substitute for RF communication due to a wide range of benefits over the RF spectrum. Till today, the interaction of metasurfaces with incident electromagnetic beams is under discussion. This work is an effort in this domain where metasurfaces have been proposed to shape the incident electromagnetic beams into vortex beams. The proposed designs can convert any polarization beam into a vortex beam. It is worth noting that the generation of ultraviolet vortex beams through metasurfaces is still an obscure idea, which has been targeted in this work. Through this work, it can be expected that the terabit/s data rate barrier can be approached in the ultraviolet regime too. This work is going to introduce nanoscale structures into free space optical communication, thereby reducing device size and increasing efficiency of operation.

REFERENCES

1. Padgett, M., J. Courtial, and L. Allen, "Light's orbital angular momentum," *Physics Today*, Vol. 57, No. 5, 35, May 2004, Accessed on: Dec. 09, 2019, [Online]. Available doi: /10.1063/1.1768672.
2. Kildishev, A., A. Boltasseva, and V. Shalaev, "Planar photonics with metasurfaces," *Science*, Vol. 339, No. 6125, 1232009–1232009, 2013, Available: 10.1126/science.1232009.
3. Genevet, P., F. Capasso, F. Aieta, M. Khorasaninejad, and R. Devlin, "Recent advances in planar optics: From plasmonic to dielectric metasurfaces," *Optica*, Vol. 4, No. 1, 139, 2017, doi: 10.1364/optica.4.000139.
4. Kuznetsov, A. I., A. E. Miroshnichenko, M. L. Brongersma, Y. S. Kivshar, and B. Luk'yanchuk, "Optically resonant dielectric nanostructures," *Science*, Vol. 354, No. 6314, 2472, 2016, doi: 10.1126/science.aag2472.
5. Hui, X., S. Zheng, Y. Hu, C. Xu, X. Jin, H. Chi, et al., "Ultralow reflectivity spiral phase plate for generation of millimeter-wave OAM beam," *IEEE Antennas Wireless Propag. Lett.*, Vol. 14, 966–969, Apr. 2015.
6. Chen, Y., et al., "A flat-lensed spiral phase plate based on phase-shifting surface for generation of millimeter-wave OAM beam," *IEEE Antennas Wireless Propag. Lett.*, Vol. 15, 1156–1158, 2016.
7. Bai, Q., A. Tennant, and B. Allen, "Experimental circular phased array for generating OAM radio beams," *Electron. Lett.*, Vol. 50, No. 20, 1414–1415, Sep. 2014.
8. Hui, X., et al., "Multiplexed millimeter wave communication with dual orbital angular momentum (OAM) mode antennas," *Sci. Rep.*, Vol. 5, 1–9, 2015, doi: 10.1038/srep10148.
9. Niemiec, R., C. Brousseau, K. Mahdjoubi, O. Emile, and A. Menard, "Characterization of an OAM flat-plate antenna in the millimeter frequency band," *IEEE Antennas Propag. Lett.*, Vol. 13, 1011–1014, 2014.
10. Yue, F., D. Wen, J. Xin, B. D. Geradot, J. Li, and X. Chen, "Vector vortex beam generation with a single plasmonic metasurface," *ACS Photonics*, Vol. 3, No. 9, 1558–1563, 2016.
11. Yang, Z., D.-F. Kuang, and F. Cheng, "Vector vortex beam generation with dolphin-shaped cell meta-surface," *Optics Express*, Vol. 25, No. 9, 22780–22788, 2017.
12. Zhang, Y., J. Gao, and X. Yang, "Spatial variation of vector vortex beams with plasmonic metasurfaces," *Sci. Rep.*, Vol. 9, No. 1, 1–11, 2019, doi: 10.1038/s41598-019-46433-z.
13. Ding, F., Y. Chen, and S. I. Bozhevolnyi, "Focused vortex-beam generation using gap-surface plasmon metasurfaces," *Nanophotonics*, Vol. 9, No. 2, 371–378, 2020, doi: 10.1515/nanoph-2019-0235.
14. Ji, C., J. Song, C. Huang, X. Wu, and X. Luo, "Dual-band vortex beam generation with different OAM modes using single layer metasurface," *Optics Express*, Vol. 27, No. 1, 34–44, 2019.
15. Zhou, H., J. Yang, C. Gao, and S. Fu, "High-efficiency, broadband all-dielectric transmission metasurface for optical vortex generation," *Optical Materials Express*, Vol. 9, No. 6, 2699–2707, 2019.

16. Yang, J., H. Zhou, and T. Lan, "All-dielectric reflective metasurface for orbital angular momentum beam generation," *Optical Materials Express*, Vol. 9, No. 9, 3594–3603, 2019.
17. Mahmood, N., et al., "Polarisation insensitive multifunctional metasurfaces based on all-dielectric nanowaveguides," *Nanoscale*, Vol. 10, No. 38, 18323–18330, 2018, doi: 10.1039/c8nr05633a.
18. Mahmood, N., et al., "Twisted non-diffracting beams through all dielectric meta-axicons," *Nanoscale*, Vol. 11, No. 43, 20571–20578, 2019, doi:0.1039/c9nr04888j.
19. Yang, Y., W. Wang, P. Moitra, I. I. Kravchenko, D. P. Briggs, and J. Valentine, "Dielectric meta-reflectarray for broadband linear polarization conversion and optical vortex generation," *Nano Lett.*, Vol. 14, No. 3, 1394–1399, 2014, doi: 10.1021/nl4044482.
20. Shen, Y., X. Wang, Z. Xie, C. Min, X. Fu, Q. Liu, M. Gong, and X. Yuan, "Optical vortices 30 years on: OAM manipulation from topological charge to multiple singularities," *Light Sci. Appl.*, Vol. 8, 90, Aug. 2019, Accessed on: Feb. 10, 2020, [Online]. Available doi: https://doi.org/10.1038/s41377-019-0194-2.
21. Hranilovic, S., "Trends and progress in optical wireless communications," *2017 Opt. Fiber Commun. Conf. Exhib. OFC 2017 — Proc.*, 26–28, 2017.
22. Sun, X., et al., "71-Mbit/s ultraviolet-B LED communication link based on 8-QAM-OFDM modulation," *Opt. Express*, Vol. 25, No. 19, 23267, 2017, doi: 10.1364/oe.25.023267.
23. Wang, J., et al., "Terabit free-space data transmission employing orbital angular momentum multiplexing," *Nat. Photon.*, Vol. 6, No. 7, 488–496, 2012.
24. Bozinovic, N., et al., "Terabit-scale orbital angular momentum mode division multiplexing in fibers," *Science*, Vol. 340, 1545–48, 2013.
25. Huang, H., et al., "100 Tbit/s free-space data link enabled by three dimensional multiplexing of orbital angular momentum, polarization, and wavelength," *Opt. Lett.*, Vol. 39, 197–200, Jan. 2014.
26. Phillip, H. R. and E. A. Taft, "Kramers-Kronig analysis of reflectance data for diamond," *Phys. Rev.*, Vol. 136, A1445–A1448, 1964.
27. Savenkov, S. N., "Jones and Mueller matrices: Structure symmetry relations and information content," *Light Scattering Reviews 4: Single Light Scattering and Radiative Transfer*, 71–114, Praxis Publishing, Chichester, U.K., 2009.